Vibrationally resolved translational energy release spectra from the ultraviolet photodissociation of methyl mercaptan

J. Segall,[a] Y. Wen, R. Singer,[b] M. Dulligan, and C. Wittig
Department of Chemistry, University of Southern California, Los Angeles, California 90089

(Received 26 February 1993; accepted 19 July 1993)

Product translational energy release spectra resulting from 248 and 193 nm photodissociation of methyl mercaptan are obtained for the hydrogen atom channels ($CH_3SH+h\nu\rightarrow CH_3S+H$) by using the high-$n$ Rydberg time-of-flight technique. The spectra exhibit vibrational structure that is assigned to a CH_3–S stretch progression. At 248 nm, the progression extends only to $v=2$, while at 193 nm levels up to approximately $v=17$ are populated. The progression observed at 193 nm is bimodal, with the higher kinetic energy component showing greater spatial anisotropy than the lower energy component, suggesting that two different processes occurring on different time scales are responsible for the two components. The results at 248 nm are consistent with excitation to a repulsive electronic surface. For 193 nm excitation, the high kinetic energy component is consistent with direct photoexcitation to a repulsive surface and/or rapid intramolecular access to a repulsive surface. The lower kinetic energy component presumably derives from the molecule spending more time on an excited surface. A simple model is applied to estimate the extent of C–S bond extension for the various processes.

I. INTRODUCTION

The product internal state distributions that derive from a photofragmentation process offer valuable insight into the potential energy surface (PES) or surfaces that govern the system as it evolves from photoexcited parent to products. In cases where more than one set of products are energetically accessible, the PES controls the branching ratios for the various product channels, as well as energy partitioning amongst the product degrees of freedom. In such cases, information gleaned in photodissociation experiments also yields insight into the corresponding bimolecular reactions that traverse the same PES.

In many cases, photodecomposition involves crossings of, and/or transitions between, adiabatic PES's. Avoided crossings can occur when two electronic configurations of the same symmetry become degenerate for a particular orientation of the nuclei; in this case, the motion of the electrons and nuclei become correlated. The dynamical consequences of this breakdown of the Born–Oppenheimer approximation has been the focus of a number of recent experimental and theoretical investigations. Accurate calculations of nonadiabatic behavior presents a significant challenge to the theoretical community.[1] Therefore, experimental information, particularly the sort that is sensitive to details of the dynamics of the system such as product energy distributions, provides a useful benchmark for theoretical calculations.

The photochemistry of methyl mercaptan, CH_3SH, has been studied extensively,[2–10] in part because it is produced in various industrial processes and released into the atmosphere.[2,8] Its absorption spectrum, as measured by Sheraton and Murray,[2] shows two prominent bands, exhibiting no discernable structure, centered around 230 and 205 nm. Early UV photodissociation studies covering the range 185–254 nm established that the dominant photochemical process leads to breaking the S–H bond:[5–7]

$$CH_3SH+h\nu\rightarrow CH_3S+H, \quad (1)$$

even though the C–S bond is considerably weaker than the S–H bond (72.4 ± 1.5 vs 86.1 ± 0.6 kcal mol^{-1}, respectively).[8(b)] These findings suggest that dissociation occurs on an excited PES, repulsive in the S–H coordinate, rather than on the ground state surface, where the weakest bond-breaking channels would be expected to dominate. Indeed, electronic structure calculations show an energetically accessible adiabatic singlet PES that is repulsive in the S–H coordinate.[11] More recent studies have measured the overall energetics of reaction (1), as well as details of the C–S bond breaking channel,

$$CH_3SH+h\nu\rightarrow CH_3+SH, \quad (2)$$

which becomes significant at excitation wavelengths below $\sim$222 nm.[8] Very recently, studies by Butler and coworkers[9,10] have indicated that the increased importance of the C–S bond fission channel at shorter wavelengths is attributable to excitation to a higher singlet PES, which is bound in both S–H and C–S coordinates. Calculations of this bound PES, along with resonance Raman spectra observed following excitation to this PES, indicate that the equilibrium C–S distance is greater on this surface than on the ground PES. Excitation to this higher adiabatic PES, they reason, leads to elongation of the C–S bond and thus increases the relative probability of reaction (2) after the system crosses to the lower excited surface, on which dissociation proceeds. It seems reasonable to suppose that excitation to this bound surface might yield a dramatically different internal state distribution of the product thiomethoxy radical, CH_3S compared to exciting the disso-

[a]Present address: Department of Chemistry, University of California, Irvine, California 92717.
[b]Present address: Department of Chemistry, California Institute of Technology, Pasadena, California 91125.

 0021-9606/93/99(9)/6600/7/$6.00

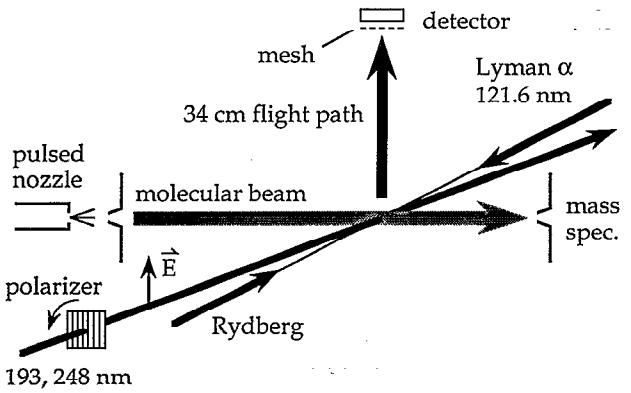

FIG. 1. Schematic representation of the HRTOF arrangement.

ciative lower surface directly. It is this aspect that we have pursued. Consequently, in this paper we report vibrationally resolved translational energy release spectra of the main channel, i.e., reaction (1), of the photodissociation of methyl mercaptan at 248 and 193 nm by using high-n Rydberg time-of-flight (HRTOF) spectroscopy.

II. EXPERIMENT

The HRTOF experiment has been described previously in some detail;[12–16] only the main points will be given here. As shown schematically in Fig. 1, a supersonic expansion of 10%–15 % CH_3SH seeded in He (stagnation pressure ~350 kPa) is skimmed and crossed with a portion of the output from an excimer laser (Questek 2820), which is weakly focused using a 1 m lens. The pulse energy of the excimer laser can be varied by a factor of 3. The photolysis radiation is polarized with a 10 plate stack of quartz slides placed at the Brewster angle and positioned such that **E** of the dissociating radiation is either parallel to the velocity vector of the hydrogen atoms that reach the detector or perpendicular to it. Referring to Fig. 1, these two cases are denoted as vertical and horizontal polarization, respectively. Experimental results show that the resultant beam is approximately 90% polarized. Hydrogen atoms are excited by VUV radiation tuned to line center of the Lyman-α transition at 121.6 nm. The Lyman-α radiation is generated by tripling the output of an excimer-laser-pumped dye laser (Lambda-Physik 3002) tuned to 364.7 nm in Kr.[17] Another excimer-laser-pumped dye laser beam (Lambda-Physik 2001), overlapping the 121.6 nm beam, transfers hydrogen-atom population from the $2\,^2P$ level to a high-lying Rydberg level (e.g., $n=40$–90). The high-n Rydberg hydrogen atoms then drift with their nascent velocities to the microchannel plate (MCP) detector, which is 33.6 cm from the interaction region. Once the excited hydrogen atoms arrive at the detector, they are easily field ionized as they pass a wire screen; they are then detected as ions. TOF spectra are recorded using a transient digitizer (DSP 2001) and averaged on a computer.

Although the detection of hydrogen atoms via the HRTOF technique allows product kinetic energy spectra to be obtained with good resolution, a drawback is that the source of the detected hydrogen is not always apparent, e.g., if there is more than one (nonequivalent) hydrogen atom present in the parent species. Even if primary photolysis products have been determined from earlier experiments, problems can result from the process usually referred to as secondary photolysis. That is, a radical species generated via parent photolysis can be photodissociated, yielding hydrogen. The effects of secondary photolysis can often be discerned by a nonlinear dependence on the photolysis fluence. However, this is not foolproof. The absence of such a nonlinear dependence does not rule out contributions from secondary photolysis, since absorption cross sections for parent and products can be very different. Therefore, care must be taken in interpreting the HRTOF spectra.

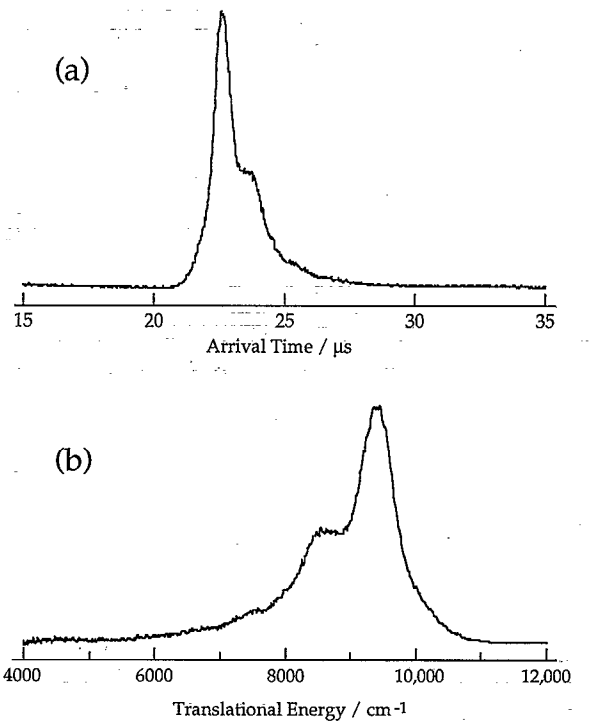

FIG. 2. (a) TOF data from the 248 nm photolysis of methyl mercaptan, 34 cm TOF tube; (b) data transformed to center-of-mass translational energy.

III. RESULTS AND DISCUSSION

The hydrogen atom TOF spectrum obtained with 248 nm photolysis is shown as an arrival-time spectrum in Fig. 2(a) and is shown transformed to a translational energy scale in Fig. 2(b). A vibrational progression is apparent, with peaks at translational energies of 9400, 8600, and 7800 cm^{-1}. The spacing between the peaks of approximately 800 cm^{-1} is compatible with literature values of the C–S stretch in the CH_3S radical of 680 ± 40 cm^{-1} (Ref. 18) and 770 ± 50 cm^{-1} (Ref. 19). We therefore assign the spectrum to a C–S stretch progression in the product thiomethoxy radical, CH_3S. Moreover, we note that the distribution shown in Fig. 2(b) is in good agreement with

distributions reported by Jensen *et al.*,[10] who detected the thiomethoxy radical. Therefore, contributions from secondary photolysis are likely to be small.

If we assume the feature at 9400 cm^{-1} corresponds to production of the rovibronic ground state of the thiomethoxy radical, these results would yield a bond dissociation energy $D_0(CH_3S\text{–}H) \sim 3.83$ eV. However, it is likely that CH_3S is formed with some rotational excitation, the magnitude of which can be estimated by taking methyl as a point mass and solving the classical equations, yielding $E_{rot}=E_{total}\ (\mu b^2)/(I+\mu b^2)$, where E_{total} is the nonvibrational energy available for products, μ is the reduced mass of the dissociating system, b is the exit channel impact parameter, and I is the CH_3–S moment of inertia. With $b=0.6$ Å, $E_{rot} \sim 0.01 E_{total}$. Therefore, our best estimate is $D_0(CH_3S\text{–}H) \sim 3.82$ eV, in reasonable accord with the value of 3.74 ± 0.03 eV reported by Nicovich *et al.*[8(b)] However, we note that care should be exercised in extracting a precise $D_0(CH_3S\text{–}H)$ value from the present data because of the rather large widths [~ 500 cm^{-1} full width at half maximum (FWHM)] of the peaks in the C–S stretch progression and the anticipated CH_3S rotational excitation imparted by the exit channel impulsive force. In contrast to the HRTOF spectrum for the 193 nm photodissociation of acetylene,[16] the peaks seen here are considerably broader than the experimental resolution, which for the present case is ~ 100 cm^{-1}. The experimental resolution is largely due to the bandwidth of the KrF photolysis laser. Therefore, there is unresolved rotational and possibly vibrational structure underlying these broad contours, adding uncertainty to the determination of $D_0(CH_3S\text{–}H)$.

It is also possible that the formation of clusters such as the methyl mercaptan dimer might also affect the observed TOF spectrum. In particular, we have observed broadening of peaks as well as tails that extend to higher translational energies.[13] We note that determination of the nascent product rotational distribution could give additional information on the angular part of the excited PES.[1] Efforts to determine what structure might be underlying the peaks in Fig. 2(b) by use of a narrower bandwidth photolysis laser are underway.

Experiments done with polarized 248 nm photolysis radiation show an order of magnitude reduction of the TOF signal when the radiation is vertically polarized, compared to when the radiation is horizontally polarized. However, only the intensity of the signal is changed. The kinetic energy release spectra observed for the two different orientations of the photolysis **E** vector are identical. The residual signal seen for horizontally polarized photolysis is almost entirely attributable to the incomplete polarization produced by the Brewster plate stack. Therefore, we conclude that the transition excited at 248 nm is very nearly perpendicular and dissociation is rapid compared to the time scale of molecular rotation, or in the notation of Zare,[20] $\beta=-1.0$. This agrees with the value reported by Jensen *et al.*[10]

The C–S stretch progression observed with 248 nm photolysis shows that the newly formed thiomethoxy radical has a C–S bond length that differs some from the equilibrium value. The observed distribution can be thought of as a Franck–Condon progression reflecting the overlap of the vibrational wave function of nascent thiomethoxy with its vibrational eigenfunctions. Although this includes all vibrational degrees of freedom, it is clear that the C–S stretch dominates. In order to obtain an estimate of the C–S bond length of the nascent thiomethoxy radical, we employed a simple harmonic oscillator model. The C–S bond of the thiomethoxy radical is modeled as a harmonic oscillator with $\nu=750$ cm^{-1} while the C–S stretch wave function in the newly created thiomethoxy radical is taken to be a displaced Gaussian whose shape is the same as that of $v=0$. The carbon-sulfur separation was varied and Franck–Condon factors were calculated. The observed product distribution was closely simulated by an increase in the C–S distance of 0.04 Å relative to its value in CH_3SH, as shown in Fig. 3. Note that the C–S bond length for methyl mercaptan has been shown to be $r_{eq}=1.81$ Å,[21] while Endo *et al.* estimate this distance as 1.79 Å for the CH_3S radical.[22] These values yield $|\langle\psi|v=1\rangle|^2=0.04$, considerably less than the $v=1$ population observed experimentally. Variations of 15% in the frequencies of both oscillators did not significantly affect the estimated C–S bond lengths. Therefore, we conclude that photoexcitation to the $1\,^1A''$ surface elongates the C–S bond, or said somewhat differently, as the system evolves on the $1\,^1A''$ surface, it experiences a force which extends the C–S bond to approximately 1.85 Å while the S–H bond is rupturing and the hydrogen atom departs. We assume that the bond length *increases*, although the model used here works equally well for contraction or expansion. However, since the excited molecule has partial $\sigma^*_{C\text{–}S}$ char-

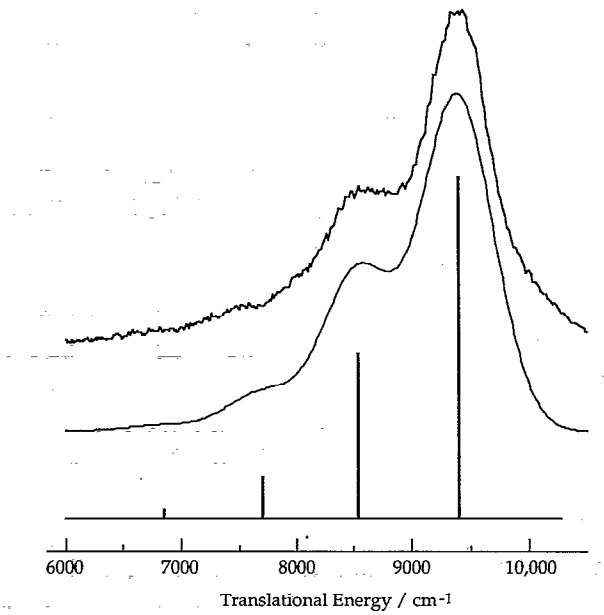

FIG. 3. Comparison between product translational energy release spectrum for 248 nm photolysis and harmonic oscillator model (see text). Traces are offset to aid viewing. Bottom trace, line spectrum from model; middle trace, line spectrum convoluted with 550 cm^{-1} Gaussian; top trace, experimental.

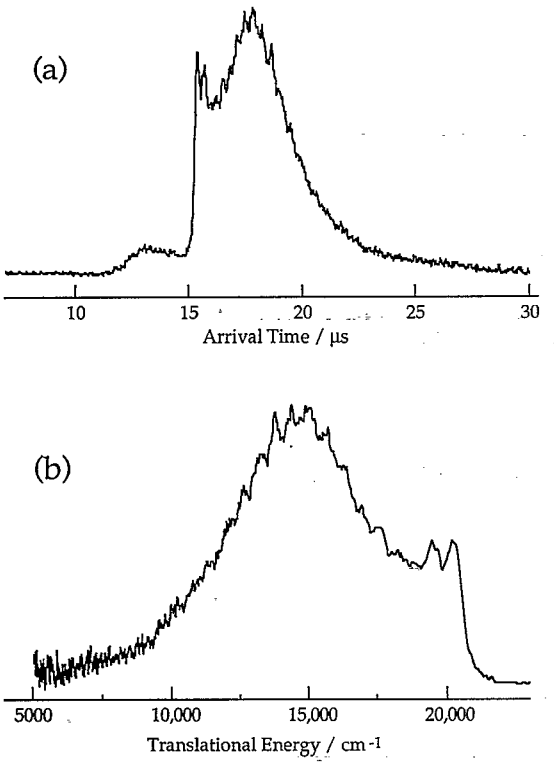

FIG. 4. (a) TOF data from the 193 nm photolysis of methyl mercaptan, 34 cm TOF tube; (b) data transformed to center-of-mass translational energy.

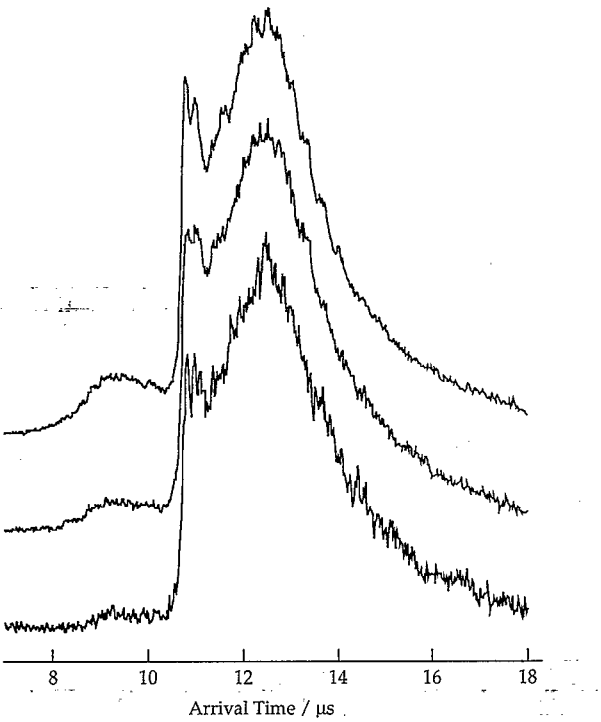

FIG. 5. TOF spectrum at 193 nm photolysis as a function of photolysis fluence. Top trace, ~1 MW cm^{-2}; middle trace, ~0.5 MW cm^{-2}; bottom trace, ~0.25 MW cm^{-2}. Absolute values are order-of-magnitude estimates, relative magnitudes are ±10%.

acter,[11] bond expansion is more physically reasonable.

This simple model does not provide a complete description of the true dynamics. Our reduction of the multidimensional $1\,^1A''$ PES to consideration of only the C–S coordinate is crude. However, the data support the idea that the C–S stretch is the most active mode in the dissociation process, and therefore the model reflects qualitatively what happens along this coordinate.

The TOF spectrum for 193 nm photolysis, as well as the corresponding translational energy distribution, are shown in Fig. 4. The fastest hydrogen atoms seen at this photolysis wavelength appear as a broad, unstructured signal in the TOF spectrum between 12 and 15 μs. This portion of the signal depends nonlinearly on the photolysis laser fluence, as shown in Fig. 5. Note that for these fluence dependence measurements, a shorter flight tube was employed and the unstructured signal is seen between 8.5 and 10 μs. This signal is most likely the result of secondary photolysis of the SH radical, as reported by Continetti *et al.* for the case of H_2S photolysis.[23] SH is known to be a photolysis product at this wavelength[9] and the signal seen here is qualitatively similar to that of Continetti *et al.* However, the unstructured signal is notably broader and extends to higher kinetic energies (4.3 vs 3.1 eV) in our case relative to theirs. This implies that the nascent HS from the photolysis of methyl mercaptan is more vibrationally excited than that created from the photolysis of H_2S. Given our findings of high C–S vibrational excitation in the dominant S–H bond breaking channel (presented later), it does not seem unreasonable to suppose that there is considerable excitation of the S–H bond in the minor C–S bond breaking channel. An alternate explanation is that all or some part of the unstructured signal is attributable to secondary photolysis of the methyl or thiomethoxy radicals.

We now turn to the structured region of the TOF spectrum, shown as a translational energy release spectrum in Fig. 4(b). The spectrum seen here is considerably richer than that obtained with 248 nm photolysis. There are two prominent peaks, reasonably well-resolved, roughly 800 cm^{-1} apart, which we will refer to below as the "fast component." This is followed by approximately 15 more poorly-resolved features, also approximately 700–800 cm^{-1} apart, which we will call the "slow component." As with the "fast component," the features of this "slow component" spectrum can be attributed to a C–S stretch progression. The main part of the progression peaks at roughly 5500 cm^{-1} from the origin, at $v=8$. Levels as high as $v=17$ can be seen. Recall that for 248 nm photolysis, $v=0$ was the dominant feature. The more extensive progression seen here is consistent with marked expansion of the C–S bond as the system evolves on the initially excited bound PES, as postulated by Keller *et al.*[9] As was seen at 248 nm, the width of the features, roughly 500 cm^{-1} FWHM, exceeds the experimental resolution at this wavelength of ~200 cm^{-1}.

As noted earlier, the possibility of contributions to the observed HRTOF spectra from secondary photolysis must be considered. In this regard, a comparison of Fig. 4 with

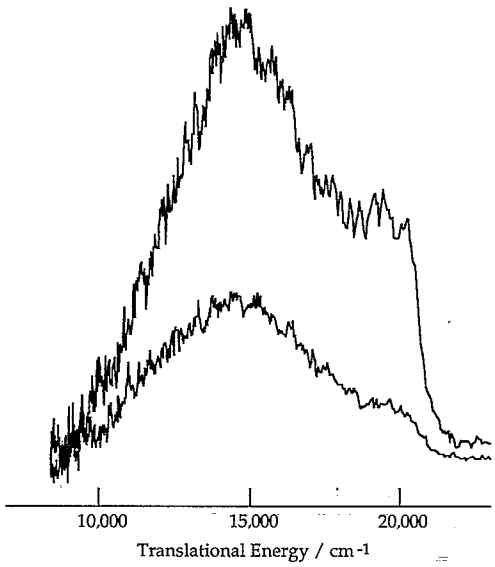

FIG. 6. Product translational energy release spectrum for polarized 193 nm photolysis. Upper trace, horizontal polarization; lower trace, vertical polarization. Vertical scale for the two traces reflects measured signal levels.

the translational energy distribution reported by Keller *et al.* (obtained by TOF of the thiomethoxy radical) reveals some differences. Though the ranges of kinetic energies observed are the same in both cases, their distribution peaks at $\sim 19\,500\ cm^{-1}$.[9] One possible explanation for this difference is that part of the signal we observe around $15\,000\ cm^{-1}$ is attributable to secondary photolysis of nascent fragments: CH_3S, CH_3, and SH. To examine this, we photolyzed CH_3SD and observed the D atom. The large "slow component" observed with CH_3SH persists; if anything, the "fast component" is diminished some. Thus, the slow component does not derive from the methyl hydrogens. Secondary SH photolysis gives fast hydrogen and displays a nonlinear dependence on photolysis fluence. Photolysis of SH to yield $S(^1D)+H$ was observed by Continetti *et al.*[23] in the photolysis of H_2S, and the fluence dependence of this channel appeared to be similar to that of the $S(^3P)+H$ channel. Therefore, any contribution to the spectrum shown in Fig. 4 from secondary photolysis is likely to be minor. This leaves open the discrepancy.

An interesting aspect of the photophysics of 193 nm methyl mercaptan photodissociation is revealed in the polarization results shown in Fig. 6. Although the fast component is observed when the photolysis radiation is horizontally polarized, it is essentially absent with vertical polarization. This is because the fast component is more anisotropically distributed than the slow component. In terms of the anisotropy parameter, we estimate $\beta=-1.0$ for the fast component (in reasonable agreement with the previously reported value of -0.85 ± 0.05°) and $\beta=-0.65\pm0.07$ for the slow component.

The observation of different spatial anisotropies for different parts of the product translational energy distribution strongly implies that there are two different processes by which the photoexcited methyl mercaptan can fragment into CH_3S+H. This is also suggested, albeit less directly, by the shape of the product translational energy distribution seen in Fig. 4(b). The bimodal intensity distribution is hard to rationalize with a single Franck–Condon progression of C–S stretch. By contrast, in Fig. 6 (in which the fast component is suppressed) the smooth rise and fall in signal intensity with increasing thiomethoxy internal energy is consistent with a single Franck–Condon progression.

One possible explanation for these observations is that there are two different electronic transitions responsible for the 193 nm absorption, and that the transition dipole responsible for the slow component is not perpendicular to the H–S–C plane. However, this is unlikely because the $2\,^1A''\leftarrow X$ transition dipole, which is thought to be responsible for 193 nm absorption in methyl mercaptan, is perpendicular to the H–S–C plane.[9,11] The reduced anisotropy of the slow component is almost certainly due to the fact that the $2\,^1A''$ surface is bound in the S–H coordinate, making dissociation slower than from $1\,^1A''$. If the dissociation time scale is not sufficiently fast compared to internal or overall molecular rotation, there is reduction in the anisotropy created in the excitation step. But this leaves us to explain the highly anisotropic fast component, which implies rapid fragmentation. One way to rationalize these observations is to assume that a part of the wave packet excited to the $2\,^1A''$ surface is able to access the $1\,^1A''$ surface rapidly, perhaps a part of the Franck–Condon region closest to the avoided crossing between the two surfaces. The remainder of the wave packet remains on $2\,^1A''$ for a longer period, during which time the C–S bond is extended, before crossing to the lower surface and dissociating. Such a combination of a direct and delayed dissociation caused by a splitting of the initially excited wave packet has been proposed before, cf. nitrosyl flouride (FNO).[24] However, the "slow" components in these cases (~ 100 fs) are still faster than the time required for molecular rotation. Alternatively, if part of the 193 nm absorption is due to a transition to the repulsive $1\,^1A''$ surface rather than entirely to the $2\,^1A''$ surface, the population transferred to the $1\,^1A''$ surface would fragment rapidly, leading to a highly anisotropic spatial distribution.

A fit of the observed 193 nm translational energy release spectrum was done following the same procedure as for the 248 nm spectrum. However, in this case, two CH_3S geometries were used, as suggested by the aforementioned discussion. First, a fit to the energy position of the peaks was made:

$$E(v)=700v-5.5v^2,$$

where the values are in wave numbers. The slow component of the distribution was fit by using a Gaussian wave packet displaced 0.27 Å from the CH_3SH equilibrium C–S length; the width of the packet corresponds to a harmonic frequency of $450\ cm^{-1}$. Attempts to model the fast component with the product state distribution seen at 248 nm yielded populations in $v=2$ and 3 that are too low, implying that the higher photon energy leads to more C–S

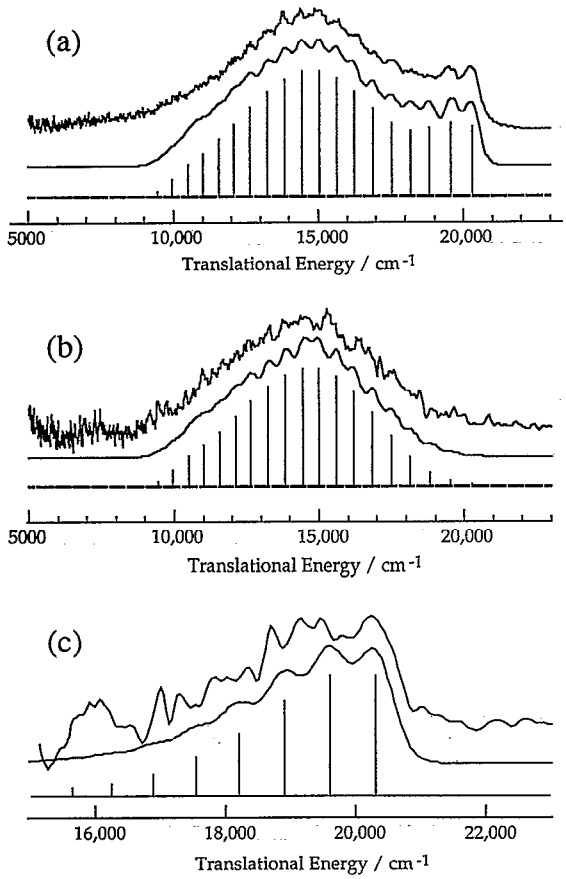

FIG. 7. Comparison between product translational energy release spectrum for 193 nm photolysis and harmonic oscillator model, as in Fig. 3. (a) Unpolarized photolysis and two excited state geometries (see text). (b) Vertically polarized photolysis, corrected for imperfect polarization and fit to slow component. (c) Difference between horizontal and vertical polarization and fit to fast component.

stretch excitation. This is probably a consequence of the higher photon energy moving the Franck–Condon region closer to the saddle point on the $1\,^1A''$ surface that separates the $H+CH_3S$ channel from the $SH+CH_3$ channel. The fast component was successfully modeled with the same Gaussian wave packet as earlier, but displaced 0.10 Å with a population equal to 21% of that of the slow component. The resulting line spectrum was convoluted with a 530 cm^{-1} Gaussian. The results are shown in Fig. 7. Although agreement with the observed spectrum is good, the model spectrum shows $v=2$ and 3 as better resolved than is seen in the experimental spectrum. This may indicate that there are different amounts of rotational excitation that result from initial excitation of the two surfaces. If so, this would reduce the structure for $v=2$ and 3, the vibrational states where both Franck–Condon progressions contribute significantly.

The Franck–Condon progressions obtained earlier can be compared to the fast and slow components directly. These spectra were obtained by taking into account the imperfect polarization resulting from the Brewster stack. The results are shown in Figs. 7(b) and 7(c).

It should be noted that product vibrational state distributions are not always well described by Franck–Condon progressions. For example, in the photodissociation of H_2S at 193 nm, a closely related system, the vibrational state distribution of the SH fragment appears to favor even vibrational states.[23,25–28] The experimental data presented here, on the other hand, support a Franck–Condon type of description. Although agreement between the measured spectra and their respective fits are good, the C–S bond distances extracted must be interpreted with care because of the crudeness of the model.

An interesting question of interpretation arises from consideration of the fact that for the slow component the dynamics transpire on two surfaces. Namely, how much of the greater C–S separation seen for the slow component is due to dynamics on the $2\,^1A''$ surface and how much to the $1\,^1A''$ surface? Or, put another way, does the C–S bond lengthening of 0.27 Å for the slow component help locate the $1\,^1A''/2\,^1A''$ avoided crossing? As the excited system evolves on $2\,^1A''$, it experiences forces which extend the C–S bond. As it approaches the local minimum on this surface, it acquires kinetic energy in this coordinate, and as it passes through the minimum, it has some probability to make a transition to $1\,^1A''$. In addition to the kinetic energy in C–S stretch, the $1\,^1A''$ surface also exerts forces to extend the C–S bond, along with the forces that lead to dissociation of the S–H bond. Therefore, C–S bond lengthening of 0.27 Å gives an upper limit for the C–S length of 2.08 Å for the region of the $1\,^1A''/2\,^1A''$ avoided crossing.

The data presented here, as well as previous results, suggest that excitation of methyl mercaptan in its second absorption band primarily accesses an initially bound state. The spatial anisotropy shows that this state remains populated for several vibrational periods. The calculations of Jensen *et al.*[10] give a hopping probability from $2\,^1A''$ to $1\,^1A''$ of 3%, also implying a $2\,^1A''$ lifetime of several vibrational periods. By comparison, photodissociation of H_2S in its first absorption band, which also proceeds via coupling of an initially excited bound surface to a repulsive surface,[28] has a dissociation time scale which is much faster. Experimental results[23,25–27] show that the spatial distribution of fragments is very close to fully anisotropic and quantum dynamics calculations on *ab initio* surfaces indicate that only a small fraction of the population remains on the upper surface after 25 fs.[28] Yet even this short residence time manifests itself in the absorption spectrum of H_2S as a symmetric S–H stretch progression.[28,29] Given the longer residence time for methyl mercaptan on its bound surface, one would expect the second band in the absorption spectrum to evince vibrational structure, most likely in the C–S stretch, as indicated by the previous discussion. However, available spectra do not show any structure in this band.[2] Possible explanations for this lack of structure are that the absorption spectra were taken at room temperature, so that hot bands wash out underlying features. In addition, it is possible that the C–S stretch frequency on $2\,^1A''$ is fairly low, making its observation difficult. Finally, motion in other parts of the molecule, such as umbrella excitation in the methyl group might also help hide the vibrational structure. Nevertheless, we expect

that spectra taken at low temperature and sufficiently high resolution should exhibit a C–S stretch progression.

IV. CONCLUSIONS

Product translational energy release spectra of methyl mercaptan photolysis at 248 and 193 nm show vibrational structure that is attributable to progressions of CH_3–S stretch. At both wavelengths, the observed widths of the features exceeds the resolution of the experiment, implying unresolved rotational and perhaps rovibrational structure. At 248 nm, the C–S progression extends only to $v=2$, while at 193 nm, levels up to $v=17$ are populated. The high translational energy "fast component" originates from a process that occurs significantly faster than the process responsible for the "slow component." The simplest explanation for these results is that the fast component arises from the repulsive $1\,^1A''$ surface and the slow component arises from the $2\,^1A''$ surface. A simple Franck–Condon model estimates that the C–S bond extends from 1.81 to 1.85 Å in 248 nm photodissociation. For the population dissociating on $1\,^1A''$ following excitation at 193 nm, we estimate the C–S distance to be 1.91 Å, while for the population evolving from $2\,^1A''$, the estimate is 2.08 Å.

ACKNOWLEDGMENTS

We thank Professor L. Butler for helpful discussions and preprints. This research was supported by the U.S. Department of Energy under Contract No. DE-FG03-85ER13363.

[1] R. Schinke, *Photodissociation Dynamics* (Cambridge University, Cambridge, 1992).
[2] D. F. Sheraton and F. E. Murray, Can. J. Chem. **59**, 2750 (1981).
[3] T. Inaba and B. de B. Darwent, J. Phys. Chem. **64**, 1431 (1960).
[4] R. P. Steer and A. R. Knight, J. Phys. Chem. **72**, 2145 (1968).
[5] A. B. Callear and D. R. Dickson, Trans. Faraday Soc. **66**, 1987 (1970).
[6] L. Bridges and J. M. White, J. Phys. Chem. **77**, 295 (1973).
[7] D. Kamra and J. M. White, J. Photochem. **4**, 361 (1975).
[8] (a) S. Nourbakhsh, K. Norwood, H. -M. Yin, C. -L. Liao, and C. Y. Ng, J. Chem. Phys. **95**, 946 (1991); (b) J. M. Nicovich, K. D. Kruetter, C. A. van Dijk, and P. H. Wine, J. Phys. Chem. **96**, 2518 (1992).
[9] J. S. Keller, P. W. Kash, E. Jensen, and L. J. Butler, J. Chem. Phys. **96**, 4324 (1992).
[10] E. Jensen, J. S. Keller, G. C. G. Waschewsky, J. E. Stevens, R. H. Graham, K. F. Freed, and L. J. Butler, J. Chem. Phys. **98**, 2882 (1993).
[11] B. Mouflih, C. Larrieu, and M. Chaillet, Chem. Phys. **119**, 221 (1988).
[12] C. Jaques, L. Valachovic, S. Ionov, E. Böhmer, Y. Wen, J. Segall, and C. Wittig, J. Chem. Faraday Trans. **89**, 1419 (1993).
[13] J. Segall, Y. Wen, R. Singer, C. Wittig, A. García-Vela, and R. B. Gereber, Chem. Phys. Lett. **207**, 504 (1993).
[14] M. N. R. Ashfold, I. R. Lambert, D. H. Mordaunt, G. P. Morely, and C. Western, J. Phys. Chem. **96**, 2938 (1992).
[15] L. Schneider, W. Meier, K. H. Welge, N. M. R. Ashfold, and C. Western, J. Chem. Phys. **92**, 7027 (1990).
[16] J. Segall, Y. Wen, R. Lavi, R. Singer, and C. Wittig, J. Phys. Chem. **95**, 0878 (1991).
[17] H. Zacharias, H. Rottke, J. Danon, and K. H. Welge, Opt. Commun. **37**, 15 (1981).
[18] P. C. Engelking, G. B. Ellison, and W. C. Lineburger, J. Chem. Phys. **69**, 1826 (1978).
[19] B. K. Janousek and J. I. Brauman, J. Chem. Phys. **72**, 694 (1980).
[20] R. N. Zare, Mol. Photochem. **4**, 1 (1972).
[21] J. H. Callomon, *Landolt-Börnstein Tables, New Series, Group II*, edited by E. Hirota, K. Kuchitsu, W. H. Lafferty, A. G. Maki, and C. S. Pote (Springer, Berlin, 1976), Vol. 7.
[22] Y. Endo, S. Saito, and E. Hirota, J. Chem. Phys. **85**, 1770 (1986).
[23] R. E. Continetti, B. A. Balko, and Y. T. Lee, Chem. Phys. Lett. **182**, 400 (1991).
[24] A. Ogai, J. Brandon, H. Reisler, H. U. Suter, J. R. Huber, M. von Dirke, and R. Schinke, J. Chem. Phys. **96**, 6642 (1992).
[25] Z. Xu, B. Koplitz, and C. Wittig, J. Chem. Phys. **87**, 1062 (1987).
[26] X. Xie, L. Schnieder, H. Wallmeier, R. Boettner, K. H. Welge, and M. N. R. Ashfold, J. Chem. Phys. **92**, 1608 (1990).
[27] G. N. A. van Veen, K. A. Mohamed, T. Baller, and A. E. de Vries, Chem. Phys. **74**, 261 (1983).
[28] B. Heumann, K. Weide, R. Düren, and R. Schinke, J. Chem. Phys. **98**, 5508 (1993).
[29] L. C. Lee, X. Wang, and M. Suto, J. Chem. Phys. **86**, 4353 (1987).